DEPARTMENT OF PHYSICS
INDIAN INSTITUTE OF INFORMATION TECHNOLOGY, DESIGN AND MANUFACTURING KANCHEEPURAM
CHENNAI - 600127

*Synopsis Of*

# $WO_3$–based Photodetectors for Optoelectronic Device Applications

*A Thesis*

*To be submitted by*

**PENNA VENKATA KARTHIK YADAV**

*For the award of the degree*

*Of*

**DOCTOR OF PHILOSOPHY**

# 1 Abstract

In photodetector technology, the bottleneck is identified as the challenges in the development of novel materials capable of detecting low-intensity electromagnetic radiation and also compatibility with the integrated circuit (IC) fabrication. Among various metal oxide semiconductors, transitional metal oxide (TMOs) based materials are more suitable for ultra-violet (UV) photodetector applications due to their wide bandgap, thermal stability, and chemical stability. In particular, tungsten trioxide ($WO_3$) has been proven to be the most suitable candidate for photonic applications including electrochromic, photochromic, and gas sensor devices.

Herein, the development of $WO_3$-based photodetector test-devices with enhanced performance has been focused. $WO_3$ thin films are deposited onto $SiO_2$/Si substrate at different oxygen partial pressure ($p_{O2}$) and sputter pressure conditions using the radio frequency (RF) magnetron sputtering technique. In the first part of the dissertation, the most vital growth parameters in sputtering techniques like $p_{O2}$ and sputter pressure for the deposition of $WO_3$ thin films are optimized based on the photodetector test-device performance. The structural, morphological, and chemical states are analyzed using various characterization techniques including X-ray diffraction (XRD), field emission scanning electron microscopy (FESEM), X-ray photoelectron spectroscopy (XPS), Raman, and atomic force microscopy (AFM). As-grown $WO_3$ thin films are used to fabricate metal-semiconductor-metal (MSM) planar structured photodetector test-device with titanium (Ti) electrodes and measured the photodetector parameters like photocurrent, responsivity, detectivity, and external quantum efficiency (EQE). The Ti/$WO_3$/Ti test-devices showed a high responsivity of 0.166 A/W under 382 nm of UV illumination at a very low power density of 0.66 mW/cm$^2$.

In order to achieve multi-spectral absorption ranging from UV to visible region, novel $WO_3$-based heterostructures are presented in the second part of the dissertation. Initially, sputter deposited graphene-based (GR/$WO_3$) heterostructures are fabricated to study the UV-visible photodetector performance. The GR/$WO_3$ heterostructures achieved a maximum responsivity of 0.085 A/W under 512 nm of visible illuminations. However, due to certain limitations of graphene, $WS_2$/$WO_3$ heterostructures are fabricated by growing $WS_2$ nanostructures onto the $WO_3$ layer by chemical vapor deposition (CVD) technique. Here, Ag/$WS_2$/$WO_3$/Ag photodetector test-device is fabricated using the interdigitated silver (Ag) electrodes. Due to the formation of nanostructures and extraordinary electron mobility of $WS_2$, the high responsivity of 2.94 A/W and 2.01 A/W is achieved under UV and visible illuminations, respectively. The obtained results attest that $WS_2$/$WO_3$ heterostructures are promising candidates for broadband UV-visible photodetectors and the same strategy can be experimented with other TMOs and TMDs to achieve a high-performance of photodetectors for optoelectronic devices.

# 2 Objectives

The objectives of this thesis are outlined as follows:

1. Optimization of oxygen partial pressure and sputter pressure growth parameters for the deposition of $WO_3$ thin films using RF magnetron sputtering technique.

2. Development of metal-semiconductor-metal (MSM) planar structured photodetector test-device for UV photodetector applications.

3. Measurement of the photodetector test-device's figures of merit (FOM) such as photocurrent, responsivity, detectivity, and external quantum efficiency (EQE).

4. Development of the $WO_3$-based photodetectors towards broadband UV-visible photodetectors by integrating it with graphene and $WS_2$.

5. Finally, the FOM of heterostructure (GR/$WO_3$ and $WS_2$/$WO_3$) based test-device samples can be evaluated for the fast optoelectronic devices.

# 3 Existing Gaps and Contributions

In the field of optoelectronic technology, photodetectors are the most crucial devices that couple the optics and electronics by interacting with the targeted optical signal or electromagnetic radiation. The most prominent component in the photodetectors is the photoactive material, which absorbs the incident light energy. Most of the traditional photodetectors have silicon (Si) as the photoactive material, since the fabrication process is scalable, allows miniaturization, and smooth integration with IC technology. However, Si-based photodetectors are facing several challenges due to their indirect bandgap, short photon penetration depth, and also being brittle. The intrinsic limitations of Si-based photodetectors motivate the investigation of novel compounds to achieve highly efficient photodetectors with extending wavelength ranges. Several interesting materials have been explored to achieve efficient absorption of target light, which includes metal oxide semiconductor such as ZnO, $TiO_2$, NiO, $SnO_2$, $WO_3$, $Ga_2O_3$, CuO, and $MoO_3$ exclusively for UV photodetector applications (Yang *et al.* (2019); Ouyang *et al.* (2019)). However, $WO_3$ is rarely reported for UV photodetector applications despite its successful use in electrochromic and photochromic devices (Huang *et al.* (2012)). In addition, $WO_3$ has a wide bandgap, it is suitable for absorbing UV radiation, and is also compatible with complementary metal oxide semiconductor technology (Qian *et al.* (2016)). Therefore, here we fabricated $WO_3$ thin films for enhanced UV photodetector applications.

There are several methods are available for the deposition of $WO_3$ thin films including spin coating, spray pyrolysis, thermal evaporation, magnetron sputtering, e-beam evaporation, and pulsed laser deposition (Chen *et al.* (2013)). Among these methods, sputtering offer a wide range of advantages including control over composition and growth, high purity films, good adhesion, and even being suitable for large-scale industrial production (Bräuer *et al.* (2010)). Henceforth, $WO_3$ thin films are deposited using the RF magnetron sputtering technique. To produce the $WO_3$ thin film-based UV photodetectors with superior figures of merit, the sputter deposition conditions are optimized by tailoring the grain size and forming the oxygen vacancies.

The UV and UV-visible photodetectors are widely used for gas sensors, flame detection, pollution sensing, bio-imaging, photoplethysmography (PPG) sensors, water quality analyzers, and microvolume spectrophotometers (Chen *et al.* (2015); Wang *et al.* (2019)). The photodetector materials used in these types of devices should be highly

sensitive to various electromagnetic spectra and also own the ability to detect very low-intensity radiation with high speed. For broadband photodetectors, metal oxide materials including $WO_3$ are inadequate due to their wide bandgap and sensitivity to a narrow electromagnetic spectrum. To address the limitations of $WO_3$ towards UV-visible detection, sputter-deposited $WO_3$ thin films have been integrated with graphene and $WS_2$ to form GR/$WO_3$ and $WS_2$/$WO_3$ heterostructures and fabricated UV-visible photodetector test-devices. Typical clinical devices take several minutes to analyze the target samples and produce the results. With the aim of achieving high response speeds, we developed MSM structured $WS_2$/$WO_3$-based UV-visible photodetector with interdigitated silver electrodes and achieved the high response speed of 100 ms.

# 4 Most Important Contributions

## 4.1 Effect of oxygen partial pressure on the UV photodetector performance of $WO_3$ thin films

$WO_3$ being an n-type semiconductor material and the number of oxygen vacancies play an important role to increase the charge carrier density. In $WO_3$ material, more number of oxygen vacancies will induce more number of charge carriers and inturn, it establishes higher photodetector performances. Therefore, in this work, the influence of $p_{O2}$ for the UV photodetector performance of $WO_3$ thin films has been studied. Here, the thicknesses of the $WO_3$ thin films are decreased from 225 nm to 150 nm by increasing the $p_{O2}$ from 5% to 20%, respectively.

From the XPS analysis, as depicted in Figure 1, it is confirmed that the $WO_3$ film deposited at 10% of $p_{O2}$ had more oxygen vacancies than the film deposited at 20% of $p_{O2}$. In W4f spectra, the peak at a binding energy of 530.50 eV is due to the presence of oxygen bonding with tungsten (W) in the $WO_3$ lattice.

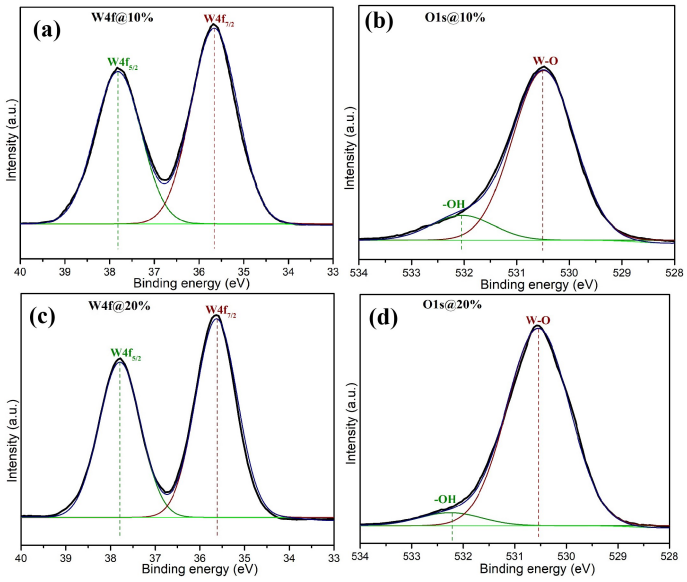


Figure 1: High-resolution XPS spectra of (a) W4f, (b) O1s at 10% and (c) W4f, (d) O1s at 20% of $p_{O2}$ grown conditions of $WO_3$ films

From the current-voltage (I-V) measurements (Figure 2) of the Ti/$WO_3$/Ti device, a linear relationship between current and voltage is observed, which implies the formation of ohmic contact between metal and semiconductor interface. The ohmic contact resulted in a narrow barrier height ($\phi_B$) at the metal-semiconductor junction, which allows the movement of free charge carriers more freely upon applying external bias, making it suitable for optical switch applications. The $WO_3$ films deposited at 10% of $p_{O2}$ show higher current under dark and UV illumination, which is contributed to the enhanced crystallanity and oxygen vaccancies.

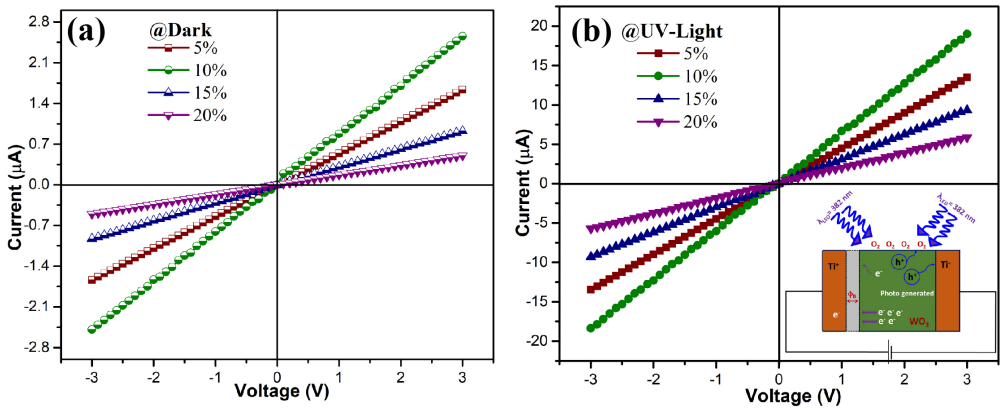


Figure 2: I-V characteristics of $WO_3$ test-device under (a) dark and (b) UV light illuminations

## 4.2 Effect of sputter pressure on the UV photodetector performance of $WO_3$ thin films

The next important parameter to fine-tune the $WO_3$ growth in magnetron sputtering is the sputter pressure. During the sputter deposition of $WO_3$ thin films, more argon (Ar) atoms are released at high sputter pressure leads to the frequent collision of the tungsten (W) atoms with other atoms (Ar and $O_2$) result to the loss of energy and thus decreases the mobility of the sputtered tungsten atoms. Hence, the films deposited at lower sputter pressure shows good adhesion and crystallinity, which will help for enhancing the photodetector properties of the test-device. The sputter phenomena of $WO_3$ film growth at high and low sputter pressure ambiances is illustrated in Figure 3.

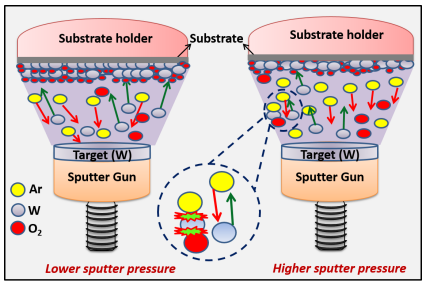


Figure 3: Schematic images of sputtering phenomena at higher and lower sputter pressures

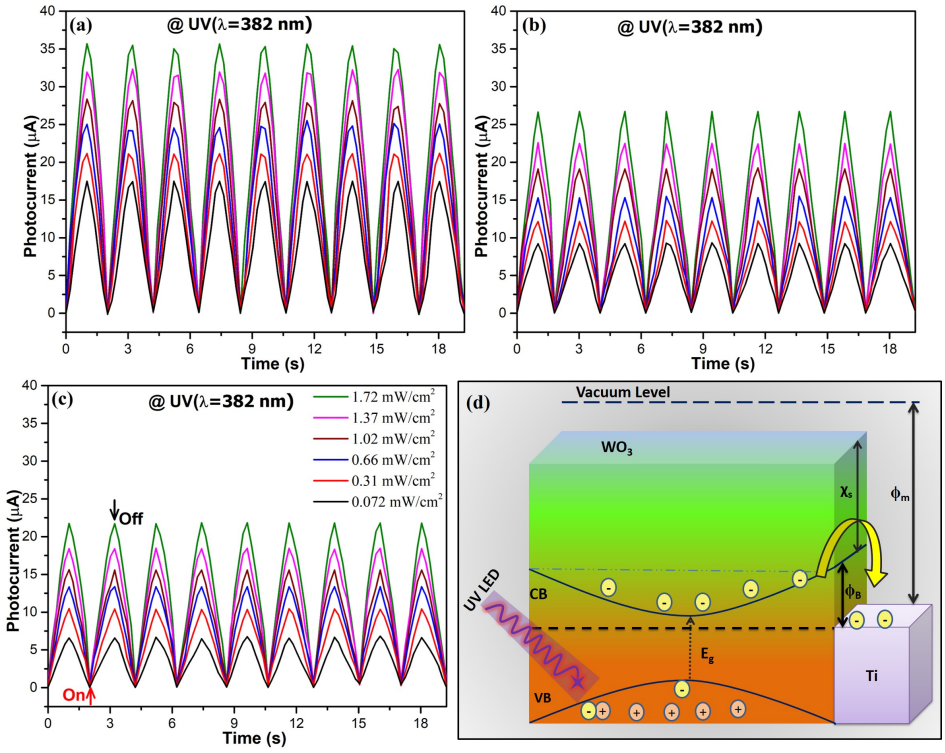


Figure 4: Photoresponse of $WO_3$ samples grown at (a) 10 mTorr, (b) 15 mTorr, and (c) 20 mTorr as a function of UV exposing time and (d) schematic energy band diagrams of $WO_3$ photodetectors under UV light illumination

In this work, the sputter pressure was optimized to deposit the $WO_3$ thin films based on the photodetector device performance. The effect of sputter pressure on the crystallinity and morphology as well as the photodetector performance of $WO_3$ films was studied. Here, the thicknesses of the $WO_3$ films were decreased from 225 nm to 95 nm as the sputter pressure was increased from 10 mTorr to 20 mTorr, respectively due to the low deposition rate upon accumulation of argon ions. The cyclic photoresponse of the $WO_3$ thin films deposited at different sputter pressures by illumination of different power densities of UV-light with an exposure time of 2 seconds are shown in Figure 4. The charge carrier generation and seperation upon UV illumination in $WO_3$ is illustrated in Figure 4(d). The excellent cyclic and stable behaviour with high photocurrent was observed for $WO_3$ films grown at 10 mTorr sputter pressure condition. The higher crystallinity, tailored grain size, and surface roughness of $WO_3$ films grown at 10 mTorr sputter pressure assist to achieve high responsivity (0.947 A/W) and external quantum efficiency (EQE: 304.20%) by minimizing the overall impedance.

## 4.3 GR/$WO_3$ heterostructure towards UV-visible photodetection

Until now, sputter-deposited $WO_3$ thin films for UV photodetector applications have been investigated. Further, to develop the $WO_3$ photodetectors toward UV-visible detection, materials with strong optical absorption in the visible region need to be integrated with the sputter-deposited $WO_3$ films. In this direction, the hybrid bi-layer of GR/$WO_3$

heterostructure was developed through the sputtering technique and Ti electrodes were deposited onto the photoactive layer for broadband UV-visible photodetector applications. The chemical state and existence of the elements of $WO_3$ and GR were confirmed from the Raman and XPS spectra.

The hybrid device of GR/$WO_3$ showed higher photocurrents of 41.82 and 12.41 $\mu$A, responsivities of 0.253 and 0.085 A/W, and detectivity of $5.136\times10^{11}$ and $1.734\times10^{11}$ Jones under the UV and visible illuminations, respectively even at lower power densities. Figure 5 represents the interface mechanism of photocurrent generation in GR/$WO_3$ heterostructures. The figures of merit under UV and visible light illuminations at different power densities onto $WO_3$, GR, and GR/$WO_3$ samples are depicted in Figure 6. The present work also demonstrated the significance of the in-built electric field through charge movement results in the higher responsivity and the importance of defects in $WO_3$, which inhibits the recombination. As a result, GR/$WO_3$ device showed the improved photodetector properties and was also tuned to detect visible light.

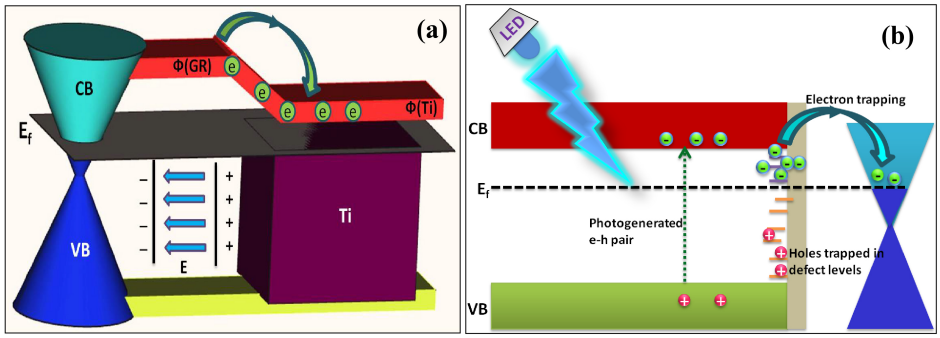


Figure 5: Schematic energy band diagrams of (a) Ti/GR and (b) GR/$WO_3$ photodetectors under UV/Vis illumination

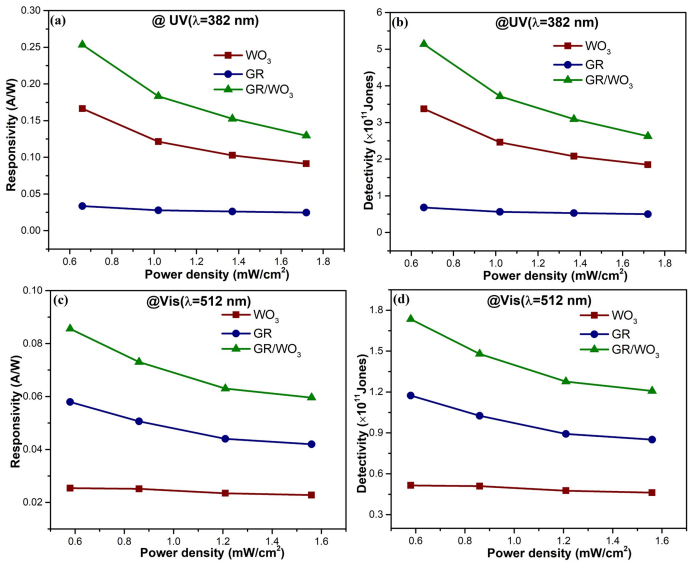


Figure 6: (a) Photoresponsivity and (b) detectivity as a function of the UV power density and (c) photoresponsivity and (d) detectivity as a function of the visible power density of $WO_3$, GR, and GR/$WO_3$ photodetectors

## 4.4 High-performance of $WS_2/WO_3$ heterostructures for UV-Vis photodetector

The zero intrinsic bandgaps of graphene and difficult fabrication methods can limit its applications in optoelectronic devices. However, the discovery of two-dimensional (2D) layered materials especially transition metal dichalcogenides (TMDs) with similar properties to graphene along with significant bandgap are found to be appropriate for optoelectronic applications. Among the TMDs, $WS_2$ is a versatile compound and suitable for ultraviolet-visible (UV-Vis) photodetector applications owing to its tunable bandgap of 2.0 eV, ultra-high mobility, higher photoluminescence, strong optical absorption, thermal stability, and operational over wide temperatures. Here, we report a strategic development of $WS_2/WO_3$ heterostructures by sputtering and chemical vapor deposition techniques to fabricate a MSM planar structured $Ag/WO_3/Ag$, $Ag/WS_2/Ag$, and $Ag/WS_2/WO_3/Ag$ photodetector test-devices with interdigitated silver (Ag) electrodes. The sulfurization of thin (10 nm) tungsten films using CVD at 800°C results in the formation of nanostructures as shown in Figure 7.

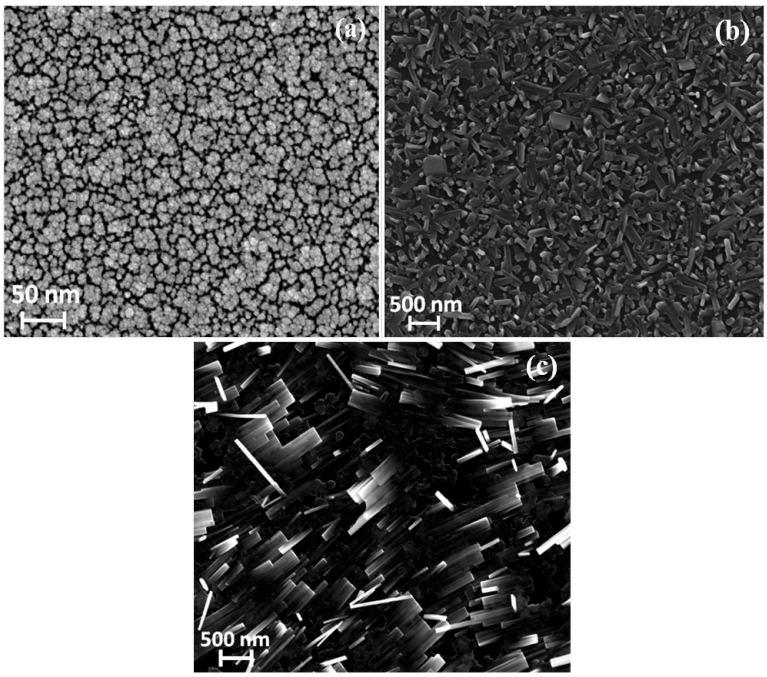


Figure 7: FESEM images of (a) sputter deposited $WO_3$ film, (b) CVD grown $WS_2$ thin film by sulfurization of thin tungsten film, and (c) bi-layer heterostructure of $WS_2/WO_3$ film

These nanostructures can enhance the photodetector test-device performance due to the increase in surface-area to volume ratio. The rapid collection of photogenerated charge carriers upon UV-visible illumination achieved a quick response time of 100 ms and the same is illustrated in Figure 8(a). Comparitively, $WS_2/WO_3$ heterostructures achieved higher photocurrent (Figure 8(b-d)) and high responsivity of 2.01 A/W even at a lower power density (0.58 $mW/cm^2$) of visible illumination. In this heterostructure, the $WS_2$ layer helps in trapping the photo excited charge carriers from the $WO_3$ and also reduces the recombination losses by absorbing the emitted radiation by $WO_3$.

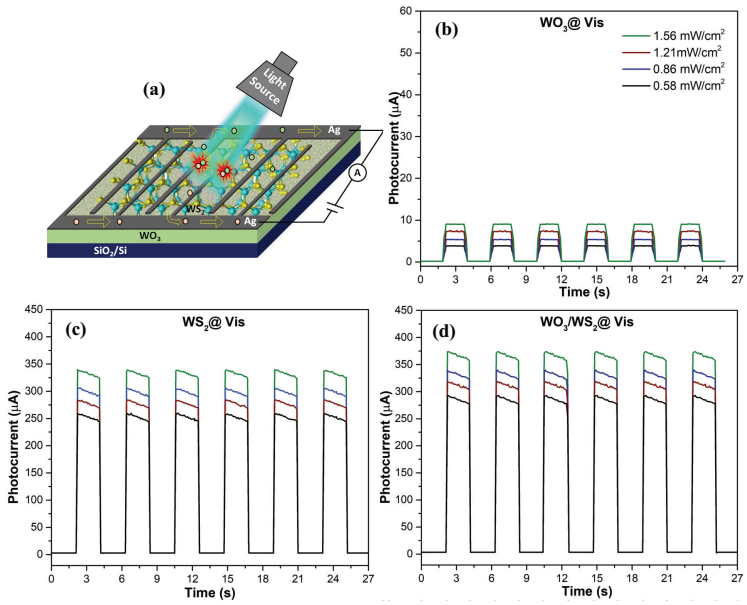


Figure 8: (a) Illustration of the quick collection of photogenerated charge carriers upon UV-visible illumination, photocurrent response of (b) $WO_3$, (c) $WS_2$, and (d) $WS_2/WO_3$ samples as a function of light exposing time at different visible light intensities

In summary, $WO_3$, GR/$WO_3$, and $WS_2/WO_3$ thin films were fabricated and analyzed the structural, morphological, and chemical nature of the as-grown thin films. The $WO_3$ growth parameters were optimized by sputtering technique at the oxygen partial pressure ($p_{O2}$) of 10% and sputter pressure (Sp) of 10 mTorr conditions based upon the superior UV photodetector performance. Further, the $WO_3$-based materials (GR/$WO_3$ and $WS_2/WO_3$) were successfully tuned towards broadband (UV-Vis) photodetectors. The figures of merit (FOM) of optimized photodetector test-devices ($WO_3$, GR/$WO_3$, and $WS_2/WO_3$) are listed in Table 1.

Table 1: The photodetector test-device properties of $WO_3$ ($p_{O2}$), $WO_3$ (Sp), GR/$WO_3$, $WS_2$ and $WS_2/WO_3$ films at 0.66 mW/cm$^2$ of UV and 0.58 mW/cm$^2$ of visible light power density illuminations

| **FOM under UV/visible light illumination** | | | | |
|---|---|---|---|---|
| **Sample** | **photocurrent (μA)** | **Responsivity (A/W)** | **Detectivity (×10$^{11}$ Jones)** | **EQE (%)** |
| $WO_3(p_{O2})$ | 27.52 | 0.166 | 3.47 | 53.56 |
| $WO_3$(Sp) | 24.02 | 0.146 | 3.05 | 47.12 |
| GR/$WO_3$ | 41.82/12.41 | 0.25/0.085 | 5.13 | 81.40/27.49 |
| $WS_2$ | 430.12/255.20 | 2.60/1.75 | 5.46 | 837.16/565.21 |
| $WS_2/WO_3$ | 489.79/296.18 | 2.94/2.01 | 14.19 | 946.76/648.52 |

# 5 Conclusions

Initially, $WO_3$-based thin films were successfully grown through the sputtering technique for UV photodetector applications. The MSM planar structured Ti/$WO_3$/Ti photodetector test-devices have been fabricated and measured the photodetector performance under UV illumination. Later, different layers (GR and $WS_2$) were introduced onto the $WO_3$ to extend the spectral absorption range from UV to visible light. In order to test this strategy, the graphene (GR) layer was deposited onto the $WO_3$ layer via sputtering technique and achieved UV-visible broadband photodetectors. Due to the specific limitations of graphene such as zero bandgap and difficult fabrication process, transition metal dichalcogenide of $WS_2$ was introduced to overcome the limitations of graphene. Herein, the $WS_2$ nanostructure layer was grown onto the $WO_3$ layer and achieved enhanced performance under both UV and visible illuminations. Further, the charge carrier transit time was reduced due to the incorporation of the interdigitated silver (Ag) electrodes and achieved a quick response time of 100 ms under both UV and visible illuminations. The acquired results confirm that the MSM planar structure with $WS_2$/$WO_3$ heterostructure device (Ag/$WS_2$/$WO_3$/Ag) can be suitable candidate for broadband and optoelectronic applications.

# 6 Organization of the Thesis

The proposed outline of the thesis is as follows:

- **Chapter 1:** Introduction
- **Chapter 2:** Literature survey
- **Chapter 3:** Experimental and measurement techniques for $WO_3$-based samples
- **Chapter 4:** Optimization of $WO_3$ sputter-growth conditions to enhance the UV photodetection
- **Chapter 5:** $WO_3$-based heterostructures for UV-visible photodetectors
- **Chapter 6:** Conclusions and future scope

# 7 List of Publications

1. **P.V. Karthik Yadav**, B. Ajitha, **Y. Ashok Kumar Reddy***, A. Sreedhar, Recent advances in development of nanostructured photodetectors from ultraviolet to infrared region: A review, Chemosphere 279 (2021) 130473.
https://doi.org/10.1016/j.chemosphere.2021.130473

2. **P.V. Karthik Yadav**, **Y. Ashok Kumar Reddy***, B. Ajitha, V.R.M. Reddy, Oxygen partial pressure dependent UV photodetector performance of $WO_3$ sputtered thin films, Journal of Alloys and Compounds 816 (2020) 152565.
https://doi.org/10.1016/j.jallcom.2019.152565

3. **P.V. Karthik Yadav**, B. Ajitha, **Y. Ashok Kumar Reddy***, V.R.M. Reddy, M. Reddeppa, M.D. Kim, Effect of sputter pressure on UV photodetector performance of $WO_3$ thin films, Applied Surface Science 536 (2021) 147947.
https://doi.org/10.1016/j.apsusc.2020.147947

4. **P.V. Karthik Yadav**, B. Ajitha,**Y. Ashok Kumar Reddy***, V.R.M. Reddy, Enhanced performance of $WO_3$ photodetectors through hybrid graphene-layer integration, ACS Applied Electronic Materials 3 (2021) 2056-2066.
https://doi.org/10.1021/acsaelm.1c00073

5. **P.V. Karthik Yadav**, **Y. Ashok Kumar Reddy***, Controlled two-step synthesis of nanostructured $WS_2$ thin films for enhanced UV-visible photodetector applications, Sensors and Actuators A: Physical (2022) (Minor Revision)

6. **P.V. Karthik Yadav**, **Y. Ashok Kumar Reddy***, Enhanced UV-visible photodetector performance by $WS_2$/$WO_3$ heterostructure, ACS Applied Materials and Interfaces (Under Review)

# References


1. **Bräuer, G.**, **B. Szyszka**, **M. Vergöhl**, and **R. Bandorf** (2010). Magnetron sputtering – milestones of 30 years. *Vacuum*, **84**(12), 1354–1359.

2. **Chen, H.**, **K. Liu**, **L. Hu**, **A. A. Al-Ghamdi**, and **X. Fang** (2015). New concept ultraviolet photodetectors. *Materials Today*, **18**(9), 493–502.

3. **Chen, H.-C.**, **D.-J. Jan**, **C.-H. Chen**, and **K.-T. Huang** (2013). Bond and electrochromic properties of $wo_3$ films deposited with horizontal dc, pulsed dc, and rf sputtering. *Electrochimica Acta*, **93**, 307–313.

4. **Huang, R.**, **Y. Shen**, **L. Zhao**, and **M. Yan** (2012). Effect of hydrothermal temperature on structure and photochromic properties of $wo_3$ powder. *Advanced Powder Technology*, **23**(2), 211–214.

5. **Ouyang, W.**, **F. Teng**, **J.-H. He**, and **X. Fang** (2019). Enhancing the photoelectric performance of photodetectors based on metal oxide semiconductors by charge-carrier engineering. *Advanced Functional Materials*, **29**(9), 1807672.

6. **Qian, K.**, **G. Cai**, **V. C. Nguyen**, **T. Chen**, and **P. S. Lee** (2016). Direct observation of conducting filaments in tungsten oxide based transparent resistive switching memory. *ACS Applied Materials & Interfaces*, **8**(41), 27885–27891.

7. **Wang, B.**, **S. P. Zhong**, **Z. B. Zhang**, **Z. Q. Zheng**, **Y. P. Zhang**, and **H. Zhang** (2019). Broadband photodetectors based on 2d group iva metal chalcogenides semiconductors. *Applied Materials Today*, **15**, 115–138.

8. **Yang, W.**, **J. Chen**, **Y. Zhang**, **Y. Zhang**, **J.-H. He**, and **X. Fang** (2019). Silicon-compatible photodetectors: Trends to monolithically integrate photosensors with chip technology. *Advanced Functional Materials*, **29**(18), 1808182.